Journal of Membrane Science 497 (2016) 229–238

Contents lists available at ScienceDirect

Journal of Membrane Science

journal homepage: www.elsevier.com/locate/memsci

Measurement of water uptake in thin-film Nafion and anion alkaline exchange membranes using the quartz crystal microbalance

V.J. Bharath [a], J. Millichamp [a], T.P. Neville [a,b], T.J. Mason [a], P.R. Shearing [a], R.J.C Brown [c], G Manos [a], D.J.L. Brett [a,*]

[a] Electrochemical Innovation Lab, Department of Chemical Engineering, University College London, Torrington Place, London WC1E 7JE, UK
[b] Centre for Nature Inspired Engineering, University College London, Torrington Place, London WC1E 7JE, UK
[c] National Physical Laboratory, Teddington, Middlesex TW11 0LW, UK

ARTICLE INFO

Article history:
Received 10 July 2015
Received in revised form
4 September 2015
Accepted 13 September 2015
Available online 25 September 2015

Keywords:
Fuel cell water management
Solid polymer electrolyte
Membrane swelling
Crystal admittance spectroscopy
Quartz crystal microbalance

ABSTRACT

Water uptake, sorption mechanics and swelling characteristics of thin-film Nafion and a commercially available Tokuyama alkaline anion exchange membrane ionomer from the vapour phase is explored using a quartz crystal microbalance (QCM). The water uptake measures the number of water molecules adsorbed by the ionomer per functional group and is determined *in-situ* using the QCM frequency responses allowing for comparison with nanogram precision. Crystal admittance spectroscopy, along with equivalent circuit fitting, is applied to both thin films for the first time and is used to investigate the ionomer's viscoelastic changes during hydration; to elucidate the mechanisms at play during low, medium and high relative humidities.

1. Introduction

Fuel cells are a promising electrochemical energy conversion technology applicable across a wide range of applications. Converting chemical energy directly into electricity with no moving parts and no point-of-use particulate or greenhouse gas emissions, they can offer higher efficiencies than current combustion engines and greater energy storage and reduced 'charge' times compared to batteries.

Fuel cells are made up of numerous components which are described in detail elsewhere [1,2]; this work focusses on the solid polymer electrolyte (SPE) ion conducting membrane. In a fuel cell, the SPE membrane serves to conduct ions (often H^+ or OH^-) between electrodes (anode to cathode in acidic fuel cells and cathode to anode in alkaline fuel cells); the membrane should also be a good electrical insulator and be impermeable to reactant species. The most common SPE membrane is Nafion (DuPont) and is used in proton exchange membrane (PEM) fuel cells, whilst advancements in alkaline SPEs has led to the first commercially available anion alkaline exchange membrane (AAEM) by Tokuyama Co. (Tokyo, Japan)

Water management in SPE membrane fuel cells is essential to achieving optimal operation; SPEs must be hydrated to allow sufficient protonic and hydroxide ion conduction in PEM and AAEM fuel cells respectively, whilst excessive liquid water will cause deleterious performance effects [3]. Water transport across SPEs is driven by several mechanisms, including diffusion by activity gradients, convection through hydraulic pressure differences and electro-osmotic drag.

Water uptake and transport through PEMs, and specifically Nafion, has been extensively studied; however, the microstructure of hydrated Nafion is currently a subject of intense study and speculation [4]; the most established theory is the Cluster-Network model presented in the 1980s [5–7]. The Cluster-Network model considers the ionomer as a network of ionic clusters formed by the sulphonic groups arranged as inverted micelles (roughly 4 nm diameter) and interconnected by narrow water channels (1 nm in diameter). Through techniques such as small angle X-ray scattering (SAXS), authors such as Gierke et al. [5] have shown that as the Nafion ionomer adsorbs water, the cluster diameter, exchange sites per cluster and number of water molecules per exchange site, all increase as shown in Fig. 1. Other publications, such as the work presented by Schmidt-Rohr and Chen [8], have shown through modelling techniques that the hydrated ionomer structure corresponds more closely to inverted-micelle cylinders with average channel diameters of 2.4 nm.

Experimental work by Zawodzinski et al. [9,10] has somewhat

* Corresponding author.
E-mail address: d.brett@ucl.ac.uk (D.J.L. Brett).

http://dx.doi.org/10.1016/j.memsci.2015.09.027
0376-7388/

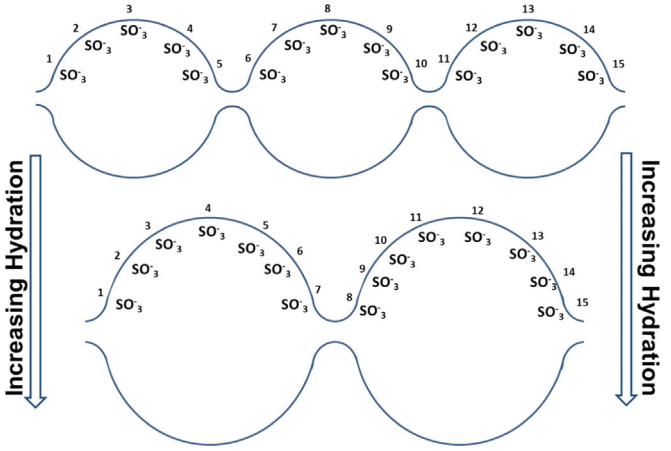

Fig. 1. : The Cluster Model theory for hydrated Nafion microstructure adapted from Gierke et al.

extended and explained the Cluster-Network model and has shown that Nafion hydrates through two distinct regimes. At low relative humidities (RHs), it is suggested that only a small quantity of water is adsorbed and the uptake corresponds to the solvation of the protons and sulphonate ions. The water in the polymer during this regime strongly interacts with the ionic components within the ionomer and these interactions help overcome the strong tendency of the polymer to exclude water due to its hydrophobic nature and swelling resistance. The second regime, which occurs at higher RHs, is thought to correspond to a large water uptake, in which the adsorbed water molecules fill the ionomer's micro-channels and result in membrane swelling.

The study of thin film (<1000 nm) Nafion ionomers has been explored in a limited capacity and remains somewhat ambiguous [4,11,12]. Characterisation work presented by Wood et al. [13] Karan and co-workers [14,15] as well as Dishari and Hickner [16] have shown the presence of an ultra-thin <55 nm hydrophilic layer developed on self-assembled thin film Nafion ionomers. The work continues to show that the water uptake values recorded at the ultra-thin film thicknesses are significantly higher and is thought to be dominated by this hydrophilicity; however, as the self-assembled layer is developed, the results show that the ionomer then exhibits more traditional hydrophobic tendencies, similar to that of bulk Nafion.

There is a growing body of literature on water management properties of AAEMs [17–19]; however, most studies have neglected to consider the transport phenomenon at the interfacial level. One of the most common commercially available AAEMs is made by Tokuyama (Japan). Whilst the exact chemical composition of the Tokuyama membrane is not certain, it is known to be made up of a hydrocarbon backbone with terminated quaternary ammonium functional groups. Many experiments have been conducted to characterise AAEM performance, durability and electro-osmotic drag [20–22] and it is proposed that as with Nafion, the ionomer hydrates and hydrophilic regions will swell, though little is understood about how AAEMs take up water or how swelling affects ion conductivity. It has been well documented that AAEMs have a significantly lower ionic conductivity than the PEM equivalent [13,14]. To compensate for this, it is common for manufacturers to introduce additional functional groups on the polymer backbone to increase the ionomer's ion exchange capacity (IEC). Excessive water loading is reported to cause mechanical instability in AAEMs [14] and consequently, the study of ionomer morphology during hydration (specifically when the ionomer is in a 'fully hydrated' state) is imperative. Similarly, improved understanding of interfacial water uptake, loading mechanisms and consequent hydroxide ion conductivity is required for AAEM ionomers. Development of AAEMs for fuel cells also needs to tackle the challenge of carbonate salt precipitation when operated in air containing CO_2 [23,24].

A promising analytical technique for the study of water uptake in thin film SPEs is the quartz crystal microbalance (QCM). Studies on Nafion have described water uptake trends and some have commented on the so-called Schroeder's Paradox [4,11,12]. However, to date, most QCM studies have limited the analysis to a simple consideration of the frequency of operation as the key metric of water uptake and overlooked viscoelastic effects, loading mechanisms and subsequent swelling of the interfacial layer upon hydration. Using the QCM to investigate viscoelastic changes of the ionomer during hydration provides potential insight into hydrated micro-structure and the links between hydration states and ionic conductivity.

This study investigates the water uptake and loading mechanisms of both thin-film Nafion and a commercially available AAEM ionomer through a range of humidities using the QCM and Crystal Admittance Spectroscopy (CAS).

2. Experimental

2.1. Ionomer water uptake

An ionomer's water uptake (λ) is defined as the number of moles of water adsorbed per mole of functional group present (mol/mol) – it is electrolyte specific. It provides a useful way to directly compare the water sorption properties of different membranes types and thicknesses; it is calculated using Eq. (1).

$$\lambda = \frac{m_w}{IEC \times m_d \times M_w} \tag{1}$$

The IEC represents the ion content per gram of polymer (mmol g^{-1}) [25], M_w the molecular weight of water m_d and m_w represent the dry membrane mass and water mass in the membrane at a given humidity, respectively [26].

Thin film ionomer m_d and m_w values differ by nanograms, and thus QCM offers a sensitive and accurate method to determine the water loading between the hydrated and non-hydrated ionomer.

2.2. Quartz crystal microbalance

The quartz crystal microbalance (QCM) is a bulk acoustic wave (BAW) resonator that has proved to be a versatile *in-situ* mass monitoring device with nano-gram resolution [27]. Bulk acoustic wave resonators contain a piezoelectric material (e.g., quartz) sandwiched between two electrically conductive metal electrodes (often gold or platinum). A voltage stimulus across the electrodes causes the quartz to resonate at a specific frequency; the frequency of this oscillation depends on the dimensions of the crystal and the amount of mass deposited on its electrodes. When there is a mass change within the system under consideration, the resultant frequency change can be accurately measured and related to a mass change using the Sauerbrey equation:

$$\Delta f = \frac{-2 f_o^2 \Delta m}{A\sqrt{\mu_q \rho_q}} \tag{2}$$

where Δf is the frequency shift experienced during mass loading, f_0 is the microbalance's fundamental frequency, A is the piezoelectric area, μ_q the shear modulus of quartz, ρ_q the quartz density and Δm relates to the corresponding mass change.

The Sauerbrey equation does however make several assumptions which can lead to limitations in its applicability, such as: any

mass deposited on the crystal is assumed rigid under oscillation and also evenly distributed across the electrode surface at a mass $\leq 2\%$ of the quartz mass [27,28]. The Sauerbrey equation assumptions also state that the deposited mass is assumed to have the same density and transverse velocity to that of quartz. The relationship assumes the frequency shift resulting from a mass deposited at some radial distance from the centre of the crystal will be the same regardless of the location [29]. Finally, when a mass or layer is added to the microbalance, it is assumed that the acoustic wave travels across the interface and propagates through the additional film – fulfilling the no-slip condition.

The QCM has been used for a range of investigations, including polymer interactions [30], and more recently in the study of the Nafion ionomer water uptake [4,11,12]. The water uptake results presented by these investigations vary and only consider the frequency shift of the QCM, so limiting the extent of information accessible using the technique. Additional insight can be derived about viscoelastic changes in the thin film by using crystal admittance spectroscopy.

2.3. Crystal admittance spectroscopy

In the normal mode of operation, the QCM is allowed to oscillate at its natural frequency and provided certain constraints are adhered to, the Sauerbrey equation provides an accurate means of measuring mass change on the crystal surface. However, the frequency response is also a function of the viscoelastic properties of the deposited material and the rheology of the surrounding environment [31]. To better understand the nature of the acoustic coupling of the crystal with a deposited layer and the surrounding environment, the frequency of oscillation can be driven across the resonance region using crystal admittance spectroscopy (CAS) [29,32,33].

The QCM device and deposited material is a composite resonator and the CAS response can be modelled using an electrical equivalent circuit. The electromechanical properties of a piezoelectric resonator can be modelled using an equivalent circuit consisting of lumped parameter elements of mass, compliance (an object's ability to yield elastically when a force is applied) and resistance based on a mechanical model of a mass M attached to a spring of compliance C_m and a piston with friction r_f, as shown in Fig. 2.

Cady [34] represented this model by a series of lumped parameters; an electrical network of inductive, capacitive and resistive components with a Butterworth Van-Dyke (BVD) circuit that represents an unperturbed crystal operating in air.

The BVD circuit can be thought of in two parts, the static and the motional arm. The motional arm (L_1, C_1 *and* R_1) is the main point of focus as it is responsible for the system's electromechanical properties. The static capacitance term (C_O) dominates the admittance/impedance away from resonance, whilst the motional arm's contribution is greatest near resonance. Fitting the circuit model to electrical measurements allows properties of the surface mass and/or liquid contacting media to be separated and

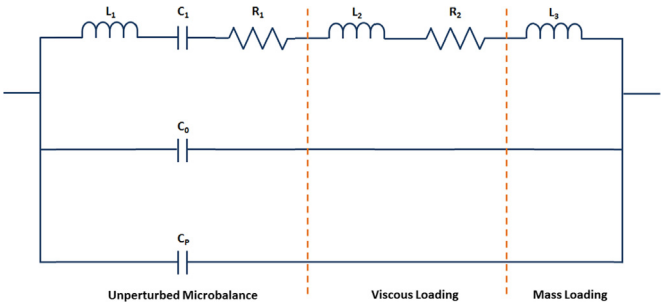

Fig. 3. : Modified Butterworth Van-Dyke equivalent circuit.

analysed. For further discussion on how the two circuits relate, the reader is referred to [29].

The BVD circuit is an accurate representation for unperturbed crystals operating in vacuum and dry gas, but requires modification for resonators in contact with a viscoelastic material [35–37]. When a QCM is in contact with a viscoelastic medium, energy passes from the crystal to the media in the form of an acoustic wave which depends on the properties of the sensor – viscoelastic interface [38].

Martin et al. [32] proposed the modified equivalent circuit shown in Fig. 3 for a QCM operating with a contacting viscoelastic phase and a contacting mass. The modified BVD introduces four new terms to the original BVD equivalent circuit:

1. For a microbalance in contact with a non-rigid medium, there is an additional inductance (L_2) and a resistance (R_2).
2. For a mass loaded crystal, a third inductance (L_3) is introduced.
3. C_p represents the parasitic capacitance and depends on the geometry of the holder and the electrode pattern on the microbalance surface.

The components used in the modified BVD represent the same physical characteristics of the QCM in the original BVD, and as such is also useful for characterisation of an unperturbed microbalance where $L_2=R_2=L_3=0$, and Fig. 3 reduces to the original BVD circuit for an unperturbed microbalance [39]. As discussed by Beck et al. [36] liquid loading causes an increase in both the motional inductance L_2 and the resistance R_2. Mass loading only affects L_3; using CAS, this model allows different frequency responses to be distinguished.

When fitting the modified BVD model, the assumptions are the same as that for the BVD, but also include: i) when the microbalance is oscillating in contact with liquid or viscoelastic media; a damped shear wave is radiated into the liquid; and ii) the contacting liquid thickness is assumed to be significantly larger than the radiated shear wave – i.e. the viscoelastic media can be assumed semi-infinite. Further information on the application and interpretation of CAS is available from [29].

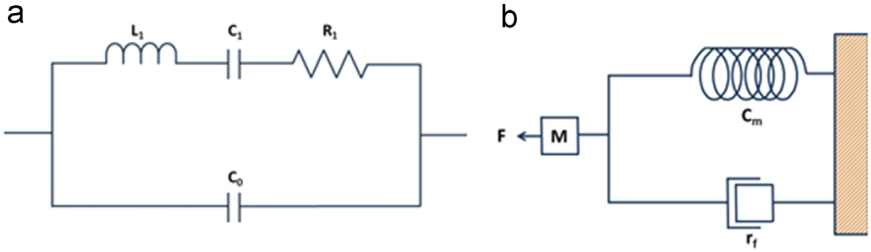

Fig. 2. : (a) Butterworth Van Dyke (BVD) equivalent circuit and (b) its corresponding mechanical representation.

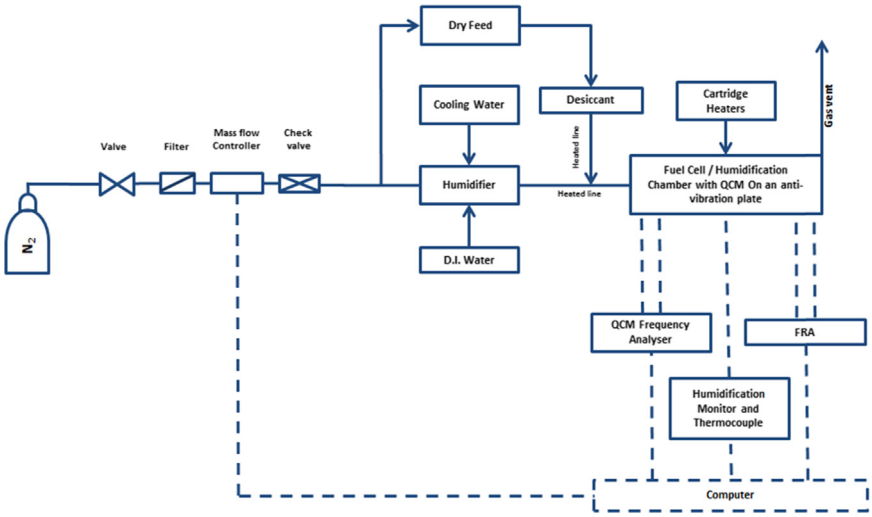

Fig. 4. : Test rig setup, with active and passive oscillation systems (the dotted and solid lines represent electrical and piping connections respectively).

2.4. Thin film ionomer casting

Thin film ionomers of both Nafion and a commercial AAEM were cast with a thickness ranging from 20–100 nm, supported on a QCM electrode. The composite resonator (QCM and ionomer) is exposed to nitrogen under a range of humidities and the consequent water uptake values and swelling characteristics determined through a combination of passive and active oscillation methods. Active oscillation measurements, in which the composite resonator's frequency response is measured when a specific voltage, were carried out using a QCM analogue controller (QCM200, Stanford Research Systems, USA). The admittance response is achieved using a Solartron 1260 impedance/gain phase analyser. Thin films are chosen for this study in order to minimise the contribution of internal water diffusion in the film [12], thus simplifying water transport analysis.

The AAEM is expected to form carbonates on contact with CO_2 (even at atmospheric concentration levels) [23,40] and so all investigations were conducted in a CO_2-free environment. Fig. 4 shows the test station developed for this investigation. The controlled humidity chamber is further described in Fig. 5a, which has a supply of dry or humidified nitrogen and is sealed to the external environment.

When casting thin films, Nafion D1021 dispersion (density 1.8 kg m^{-3}[11]) (DuPont, USA) and Tokuyama AS4 (density 0.94 kg m^{-3}) (Tokuyama, Japan) were used respectively. Ionomer dilutions were made using methanol and IPA for the Nafion and AAEM electrolytes respectively and cast onto gold coated double-anchor electrodes, on 6 MHz AT-cut 14 mm diameter QCMs (Inficon).

In the casting process, dispersions of each ionomer were applied *in-situ* to the crystal surface via a micro-pipette; the dispersed solutions dried under a stream of non-humidified nitrogen to leave a cast ionomer. The Nafion ionomer was cast and operated at 80 °C, whilst the AAEM was kept at 50 °C to limit the effect of nucleophilic displacement and subsequent membrane degradation, which is reported to occur around 60 °C [25,41,42].

The dry membrane thickness can be determined using the Sauerbrey Eqs. (2) and (3) below:

$$t_i = \frac{m_i}{A \times \rho_i} \tag{3}$$

where t_i is the ionomer thickness, m_i is the ionomer mass (determined from the Sauerbrey Equation), A is the cast area and ρ_i the density of the recast ionomer.

The cast was confined to the centre of the double-anchor electrode using the O-ring in the top of the QCM holder, shown in Fig. 5b. This allows continuity across all experiments as the cast is kept to a specific area and reduces the risk of spurious radial mass loading which produce non-ideal frequency responses and also allows determination of the film thickness.

As with other thin film ionomer studies [4,11,12], this investigation uses thin-film ionomers with thicknesses ranging from 20 nm to 100 nm. Ionomers within this range were chosen in order to minimise contribution from internal water diffusion, as discussed; but also to ensure they were within the operating range of the QCM. For the first time in an ionomer-QCM investigation,

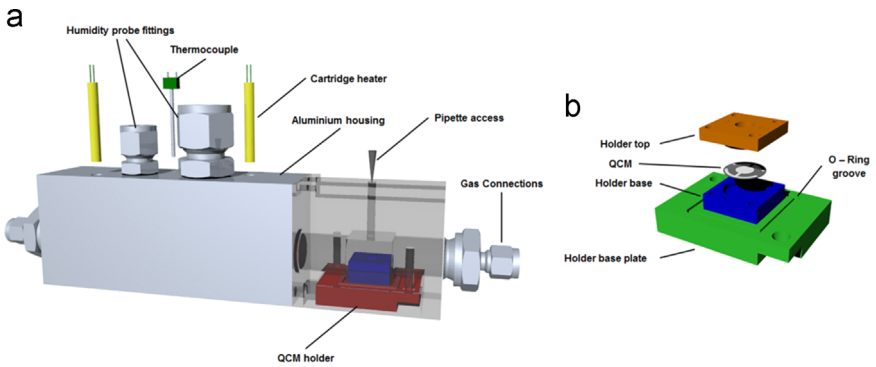

Fig. 5. : (a) The fuel cell humidification chamber, with *in-situ* casting chamber shown in the translucent section, and the QCM holder. (b) The holder shown in greater detail with QCM resonator and base plate for attachment to the humidification chamber.

this study implements CAS; this allows determination of whether the cast ionomer operates within the QCM passive oscillation range. If the contacting viscoelastic ionomer is too thick, the composite resonator becomes overly capacitive, and is therefore unable to achieve a real resonant frequency [43].

The QCM holder is designed and manufactured in-house from one piece of unfired pyrophyllite, with electrical connections to each electrode, and encompasses an internal O-ring (not shown) to confine the cast area to the centre of the microbalance's top electrode. The holder (Fig. 5b) clamps the QCM from above and below, ensuring repeatable compression, good electrical connection and frequency stability. The electrical connection between the QCM and the frequency analyser was made using platinum wire and mesh. The holder sits on a metal plate which along with a further (external) O-ring is used to seal the cell within the chamber.

The QCM holder is housed within the body of the humidified cell (Fig. 5a) and contains an access point for *in-situ* casting. Similar investigations [4] have cast the ionomer *ex-situ* and operated the microbalance under humidified environments; however, as this investigation includes the AAEM, *in-situ* casting was imperative to avoid the effect of CO_2. The drop cast ionomer's uniformity is inspected visually to ensure it fully covers the centre electrode and this has also been checked using SEM to ensure the thin film is evenly distributed preventing both a misreported thicknesses and spurious radial mass loading on the microbalance.

3. Results and discussion

3.1. Nafion water uptake

3.1.1. Active oscillation – frequency response

Fig. 6 inset shows the microbalance frequency response for a 33 nm cast Nafion membrane operating over a range of RHs. The decreasing resonant frequency response with increased humidity is consistent with an increase of mass (electrolyte wet mass) loading on the crystal microbalance. Note that the initial exaggerated frequency drop is a result of a feed stream valve switching between the dry and humidified gas supply. If we initially assume that the Sauerbrey equation holds as an accurate measure of mass of water added to the layer, Eq. 1 can be used to determine the membrane's water uptake at a given humidity using the differences between its dry mass, wet mass and its IEC. The result for a 33 nm and a 60 nm thick membrane is shown in Fig. 6.

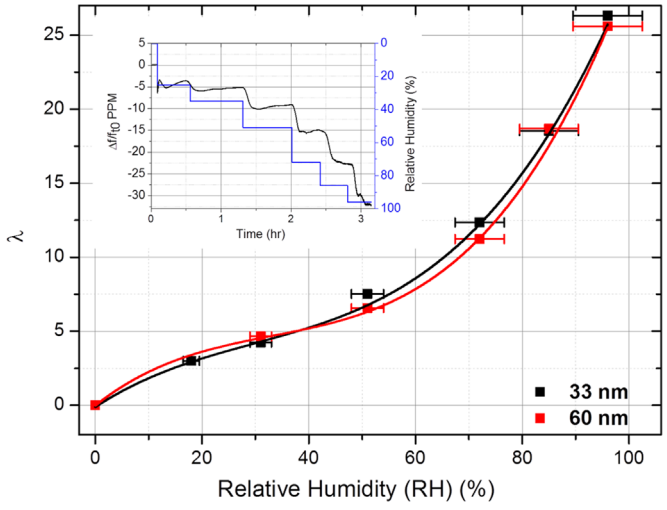

Fig. 6. : Nafion ionomer water uptake for 33 nm (black line) and 60 nm (red line) thick ionomers operating through a range of RHs. The composite microbalance's (33 nm) frequency response when operating in humidity is also shown (inset) (For interpretation of the references to colour in this figure legend, the reader is referred to the web version of this article).

Many sources confirm an increased Nafion water sorption and subsequent swelling with increasing RH; the more water in the operating environment, the greater the swelling (up until the point of maximum hydration) [3,4,11,44].

As the contacting nitrogen's RH is increased, the resonant frequency decreases; this process is understood to be instantaneous [12] however, as can be seen, frequency stabilisation takes some time in this case. The frequency stabilisation period is directly attributed to the equilibration of the membrane water content with the operating atmosphere – the extended equilibration time can be accredited to the dew point humidifier PID control.

The water uptake for a 33 and 60 nm electrolyte is reported in Fig. 6, and both electrolytes show good agreement to one another and to published literature, following the third-order polynomial trend for Nafion water uptake at specific RHs [3,4,11,44].

The Nafion water uptake values obtained at higher ($>70\%$) RHs in this investigation are higher than some presented by other authors for studies also conducted in the vapour phase [4,10,12]; the anomaly between the uptake in the liquid and vapour phase is commonly attributed to Schroeder's Paradox [45]. Schroeder's Paradox is a phenomenon used to describe the difference in solvent uptake by a polymer when exposed to saturated vapour and pure liquid. However, work presented by many authors, including Zawodzinski et al. [10], has been unable to fully understand why Schroeder's Paradox affects the Nafion ionomer and have explained the issue as a result of experimental set up, procedure discrepancies, time frames and have also ruled out the effect of sorption kinetics. The water uptake results presented here in the vapour phase at the highest relative humidities are comparable to those often achieved in liquid phase investigations [3,10] and, not for the first time show little or no contribution from the Schroeder's Paradox effect [46,47]. The use of CAS will help understand this effect.

Nafion is expected to be fully hydrated at a water uptake value of $\sim$22 [3,10]. Work by Krtil et al. [11] has shown that this value is obtained using a cast QCM in humidified nitrogen at a RH near 100%; however, in this case these values are obtained around 92% RH, according to Fig. 6. This variation can be attributed to instrumentation accuracy (dew point humidifier accurate to $\pm$ 1.5 °C) and limits in the use of the Sauerbrey equation applied to this system. Crystal admittance spectroscopy provides a more robust analysis of crystal loading than the Sauerbrey equation affords.

3.1.2. Passive oscillation – crystal admittance spectroscopy (CAS)

Fig. 7a shows the Nyquist plot for the cast Nafion composite resonator through a range of RHs. The Nyquist plot can help delineate the effects of contacting rigid mass and viscoelastic properties of the composite resonator. The resonator's magnitude of admittance response is shown in Fig. 7b, and is the plot most often used to describe such a system's properties.

As the membrane hydrates, the general trend observed is that the diameter of the admittance locus decreases and the magnitude of the admittance plot shifts to a lower frequency, with a decrease in amplitude ($|Y|_{max}$). This is indicative of increased resistance in R_2 and suggests an increasingly viscoelastic contacting media. For further reference and supplementary theory on how to interpret the admittance data, the reader is referred to [29,32,38]

The $|Y|_{max}$ peak describes the effect that humidity has on the viscoelastic properties and occurs at the series resonant frequency (f_s). Fig. 8a and b further emphasises the effect that hydration has on the magnitude of admittance by plotting the change in frequency at which the $|Y|_{max}$ value occurs (f_s) and the value of $|Y|_{max}$

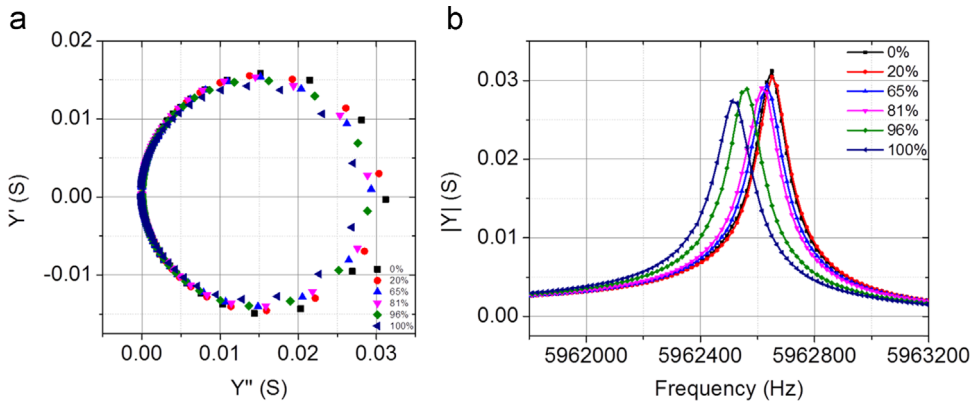

Fig. 7. : CAS response for a 33 nm Nafion composite resonator operating through a range of RHs and hydration states: (a) admittance locus (systems susceptance (Y') against conductance (Y'')) and (b) magnitude of admittance Bode plot.

through the range of operating RHs, compared to the value at 0% RH respectively.

Initially, at RHs < 35%, Fig. 8a shows no change in the series resonant frequency with increasing RH; however, Fig. 8b shows that the amplitude of the $|Y|_{max}$ peak decreases steadily by 8%. The reader is directed to literature such as [29] for further reference on understanding the nuances CAS; but because of the nature of CAS, when measurements are taken across a frequency range, the frequency response reported in Fig. 8a includes a quantisation factor and is thus low resolution and should be used only as a supplementary to the active oscillation response as a guide. Together, plots of this nature indicate that there is little additional mass, but an increase in the composite resonator's viscoelastic component. When compared to the magnitude responses between 35–96% RH, it can be seen that the composite resonator continues to load water, but in this case the loading has a significantly less viscoelastic effect on the resonator with increasing RH; this is represented by a steep change in f_s by 90 Hz and the corresponding slow-down in the percentage change of only 8.5% across the period, as seen in the $|Y|_{max}$ plot shown in Fig. 8b. The reader is reminded that perfect rigid loading (i.e. no viscoelastic effect) will see a consistent $|Y|_{max}$ amplitude, with a decreasing resonant frequency corresponding to the mass of the contacting species – relatable using the Sauerbrey Equation. Above 96% RH, there is a sharp decrease in the resonator's f_s (50 Hz) and $|Y|_{max}$ (9%) amplitude, as represented in Fig. 8a and b respectively. This change is commonly referred to as an additional viscous loading; such as a contacting liquid, e.g. water.

The magnitude of admittance plots clearly indicate the presence of two loading regimes; one at low RHs in which there is limited water uptake (constant f_s) but large viscoelastic changes in the Nafion membrane, followed by a larger water uptake with more rigid-type loading characteristics at higher RHs. Following these loading regimes, the sharp decreases in f_s and the $|Y|_{max}$ amplitude are likely to be due to contacting water on the hydrated membrane's surface. The presence of two distinct loading regimes coupled with the water uptake plots shown in Fig. 6, is consistent with the theory discussed by Zawodzinski et al. [10], which showed water loading to occur in two regions (ion solvation followed by micro-channel hydration and swelling [43]). It must be noted here that though it is suggested that the solvation and swelling regimes dominate with increasing RH respectively, there will be elements of both mechanisms at all RHs as shown by previous Environmental Ellipsometric Porosimetry studies [4]. Both Fig. 8a and b show that above 96% RH the membrane's viscoelasticity increases significantly – even more so than the initial loading regime. This large change in the composite resonator's viscoelasticity is likely due to contacting liquid water on the composite resonators surface as the membrane becomes fully hydrated and cannot further load any water. This coincides with roughly the same RH at which the predicted maximum hydration occurs (water uptake $\lambda = 22$ [3,10]), seen in Fig. 6.

Upon fitting the admittance response using the equivalent circuit shown in Fig. 3, the value of different components of the equivalent circuit can be derived. Specifically, R_2 and L_2 allow elucidation of the membranes viscoelastic properties (Fig. 9). L_1 and L_2 are indistinguishable and are often lumped for simplicity of fitting and the R_2 value is often used to directly distinguish between changes in the composite resonator's viscoelastic properties [43].

Fig. 9 initially shows that as the RH is increased to 35%, R_2 increases steadily by 1 Ω as the ionomer becomes more viscoelastic.

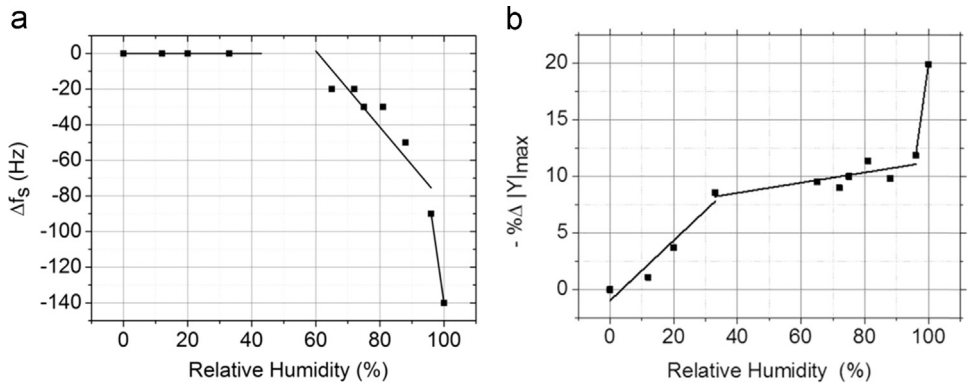

Fig. 8. : (a) Series resonant frequency and (b) percentage decrease in the amplitude of admittance as a function of RH for a 33 nm Nafion composite resonator (linear sections added as a guide to the eye).

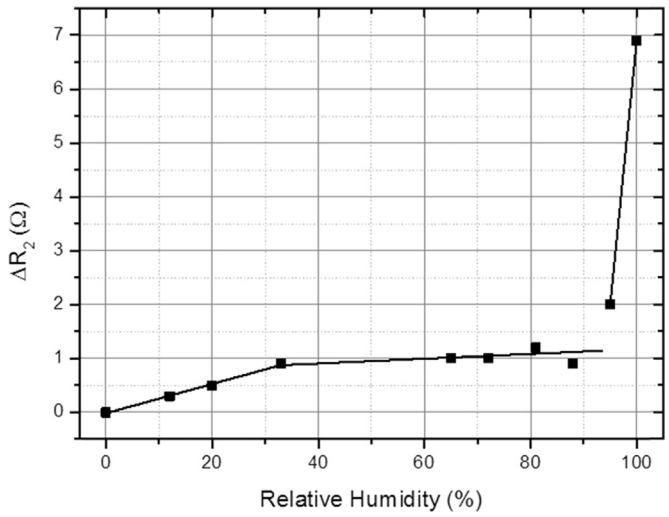

Fig. 9. : Change in composite resonators resistance (R_2) in the modified BVD equivalent circuit as a function of RH (linear sections added as a guide to the eye).

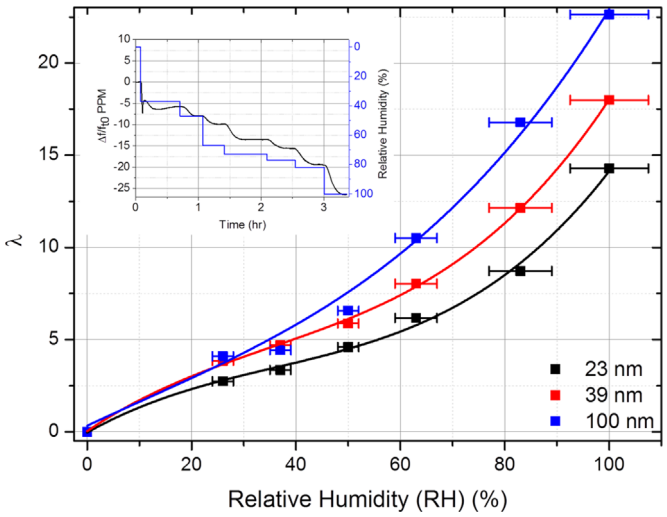

Fig. 10. : AAEM ionomer water uptake for a 23 nm (black), 39 nm (red) and 101 nm (blue) thick ionomers operating through a range of RHs. The composite microbalance's (39 nm) frequency response when operating in humidity is also shown (inset) (For interpretation of the references to colour in this figure legend, the reader is referred to the web version of this article).

Beyond 35% RH it can be seen that the rate of resistance change decreases significantly, increasing by only 0.2 Ω up until the RH reaches 88%. Though R_2 doesn't vary significantly between 35% and 88% RH, it must be noted that there are still loading processes occurring on the membrane, as discussed and demonstrated in Figs. 6 and 8.

Finally, above 88% and specifically 96% RH, R_2 increases sharply – this indicates a significant increase in viscoelasticity of the composite resonator. The sharp change observed in the composite resonators R_2 and consequent viscoelasticity supports the data seen in Fig. 8a and b, and is significantly sharper than the R_2 changes seen previously; this suggest the presence of a contacting liquid; whether that liquid water is contacting on the ionomer/nitrogen or gold/ionomer interface still remains unclear.

3.2. Anion alkaline exchange membrane

3.2.1. Active oscillation – frequency response

As with the Nafion water uptake calculations, both the dry and wet mass of the membrane must be known in order to determine the AAEM's water uptake. Once again, in order to determine the mass of the wet membrane, a cast AAEM (39 nm) QCM is operated under variable RH environments; the resulting frequency response is then recorded, as shown in Fig. 10 (inset).

The frequency trend observed is similar to that of Nafion in that increasing RH results in a reduction of the QCM's resonant frequency. Again, as the valve is switched from the dry nitrogen stream to the humidified stream, there is an initial sharp frequency drop artefact. Fig. 10 shows the water uptake values determined experimentally for AAEMs of 23 nm, 39 nm and 100 nm thickness; as with Nafion, the results here also follow a third order polynomial trend.

Whilst not extensively tested, some literature pertaining to commercial sheet AAEMs does exist [48,49] and results indicate lower water uptake values compared to Nafion, as observed here. The third-order polynomial water uptake trends are comparable to those published by Li et al. for sheet AAEM [26]; however, there is no information on the effect the thickness of the cast AAEM has on its water uptake. Fig. 10 shows that at lower RHs ($< 50\%$) there is only a small difference in water uptake for different membrane thicknesses; however, at higher RHs ($> 50\%$) the thicker membranes exhibit greater water uptake. The reason for this discrepancy is still unclear, but could be a result of interaction of the ionomer with the electrode, constraining the film from swelling and absorbing water; or alternatively the formation of a water impermeable layer as a result of disordering of channels at the gas/ionomer interface.

The results presented in Fig. 10 suggest a lower water uptake for AAEM than Nafion, with comparable thickness – this compares well with published literature [22,49,50], all of which report water uptakes between 18 and 20 when operated in water. It is important to note that the frequency response shown in Fig. 10 (inset) indicates very similar levels of water on the QCM surface; however the AAEM with a much higher IEC results in a lower water uptake per exchange site. The difference in uptake values is likely due to the variance in wettability of the main chains (the polytetrafluoroethylene polymer backbone in Nafion and the hydrocarbon polymer backbone in the AAEM) and side chains (the sulphonic acid group and the quaternary ammonium group in acid and alkaline membranes), respectively [26].

AAEM swelling reports are scarce, and those available are for studies investigating in-house fabricated AAEMs. However, literature from Li et al. [26] has suggested from *ex-situ* testing that the commercial AAEM thickness remains almost unchanged during the water uptake process; whereas Nafion increases by almost 40% when fully hydrated [51].

The theory presented by Li et al. can be explored using the QCM and CAS. Following the work presented on Nafion and the Cluster-Network model, it is understood that as the membrane swells, its viscoelasticity will slowly increase in-line with the operating RH [43], after some period of ion solvation (rapid viscoelastic effects). However, theoretically, if there is very little change in the membrane thickness during the water uptake process (i.e. no swelling – as predicted by [26]), there should be negligible viscoelastic change, and hence no change in the system's R_2 or $|Y|_{max}$ amplitude, but instead only in f_s.

3.2.2. Passive oscillation – crystal admittance spectroscopy (CAS)

Fig. 11 shows the admittance responses for the cast AAEM composite resonator operating through a range of RHs.

The AAEMs Nyquist and Bode plots at different RHs are shown in Fig. 11a and b, respectively; as with Nafion it shows that increasing RH results in a decreasing admittance locus diameter – albeit with significantly bigger shifts than with Nafion. The Bode plot shows that while the frequency decreases with increasing RH, the decrease in $|Y|_{max}$ amplitude is very significant, and again

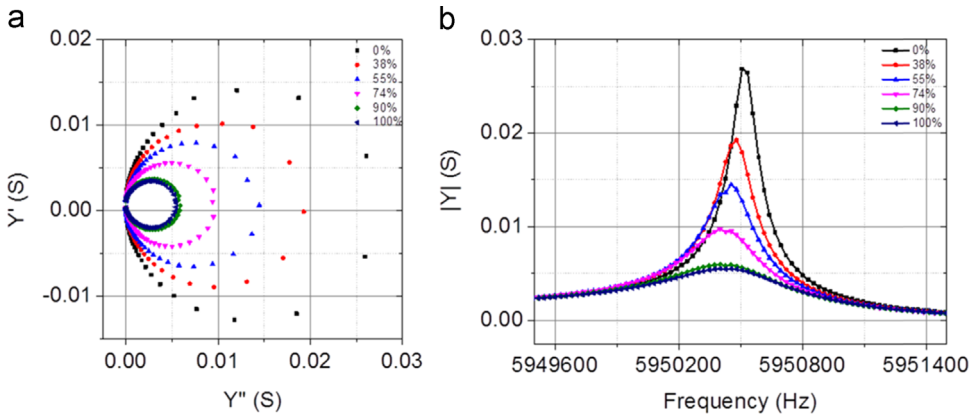

Fig. 11. : CAS results for a 39 nm AAEM composite resonator operating through a range of RHs and hydration states: (a) Admittance locus and (b) magnitude of admittance plot.

much greater than for Nafion, this is further explored in Fig. 12.

The understanding of how AAEMs respond to humidification is still ambiguous with scarce and yet conflicting literature available. However, once more, the changes observed in the magnitude of admittance plot generally indicate viscoelastic loading effects with increased humidification. Fig. 12a and b show the composite resonator's series resonant frequency (f_s) and the percentage change in the amplitude of the magnitude of the admittance peak, respectively. As suggested in Section 3.1, the initial Nafion water loading relates to the ionomer ion solvation below 35% RH; this is represented by low levels of water sorption, that increase the composite resonators viscoelasticity. The AAEM sees a similar trend; however, this initial 'viscoelastic dominant/ion solvation' loading mechanism extends over a wider range, from 0 to 85% RH. Above 80% RH, the resonant frequency remains constant, comparing this to the magnitude of admittance peak amplitude is very telling; it shows that as the RH is increased between 0–88% the amplitude of the $|Y|_{max}$ decreases significantly – to roughly 80% of the original value. However, $>88\%$ RH, the rate at which the amplitude of $|Y|_{max}$ slows significantly and only drops by 2.5%. The reader is reminded that Fig. 12b shows the resonant frequency for the CAS response; this quantisation factor renders the response to low resolution and should be used only as a supplementary to the active oscillation response for a guide. Coupled with the trends seen in Figs. 10 and 11, where it is clear that the membrane is still loading water, it can be suggested that this later 'more rigid type' loading mechanism can be attributed to the membrane swelling [43] – similar to that seen in the Nafion ionomer above 35% RH. Unlike Nafion, the suggested membrane swelling region is a small RH window, with very little change in f_s, which indicates small ionomer swelling, supporting the theory of Li et al. [26]

The AAEM admittance response suggests the presence of two loading regimes – similar to that of Nafion (excluding the proposed contacting water on the Nafion ionomer). As with Nafion, the AAEM's initial loading regime has significantly larger viscoelastic effects on the membrane when compared to that of the second regime; this presents a significantly more rigid-type load to the composite resonator. Unlike the Nafion membrane, the AAEM does not exhibit effects of contacting liquid water, even at the highest RHs, which indicates that the membrane may still be undergoing hydration and swelling.

The authors believe that the results could be suggestive of a modified version of the two-stage Nafion water loading mechanisms presented by Zawodzinski et al. [10] The AAEM ionomer is reported to have significantly more functional groups compared to Nafion, to compensate for a shortfall in its ionic conductivity; thus the ion solvation process is likely to require significantly larger quantities of water molecules to overcome the ionomer's hydrophobic nature, and consequently leads to a large decrease in f_s compared to Nafion. At higher RHs, the change in the resonators viscoelasticity decreases significantly and suggests, as with Nafion, a period of ionomer swelling – the corresponding Δf_s is 0 and indicates negligible water loading – this may suggest that the quantity of water loaded for ionomer swelling is greater for Nafion than the AAEM ionomer.

The R_2 fit data is shown in Fig. 13 for the ionomer water uptake through a range of RHs. Initially the resistance increases very steadily up to 80% RH, showing a large viscoelastic change in the composite resonator, corresponding well with Figs. 10–12. Between 80% and 85% RH, there is a sharp resistance change of 50 Ω and this represents a large increase in the resonator's viscoelasticity. Above 85% RH, the R_2 rate of increase slows considerably

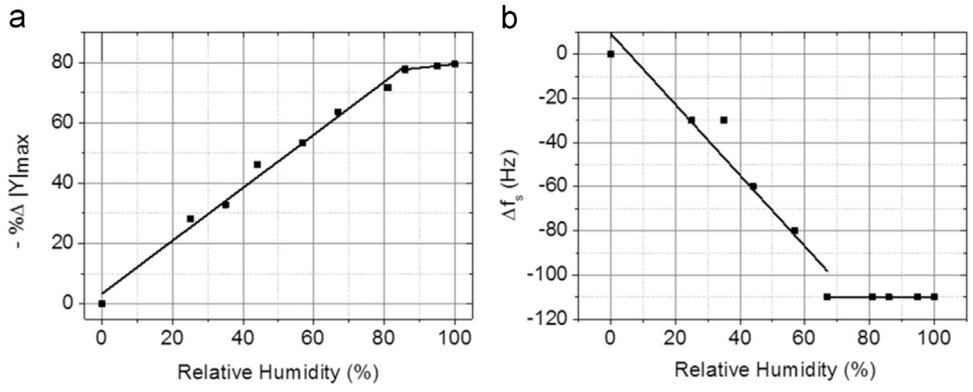

Fig. 12. : (a) Series resonant frequency and (b) percentage decrease in amplitude of admittance for a 39 nm AAEM composite resonator versus RH and hydration (linear sections added as a guide to the eye).

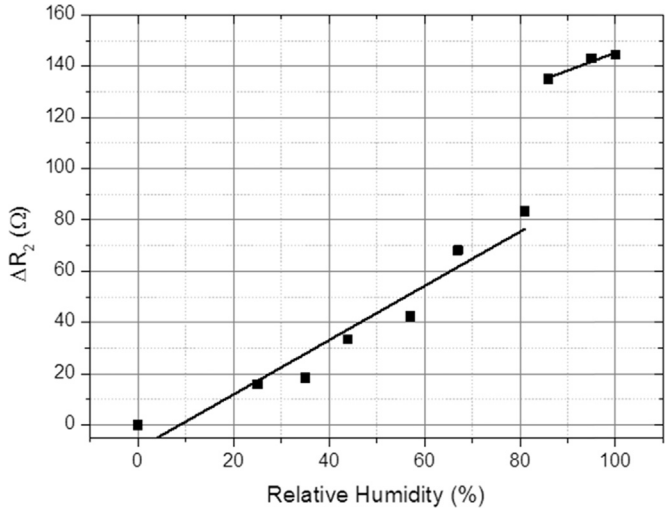

Fig. 13. : Change in composite resonators resistance (R_2) in the modified BVD equivalent circuit as a function of RH (linear sections added as a guide to the eye).

through to 100% RH. As with Nafion, the slow-down in the rate of increase of R_2 is suggestive of a period of low viscoelastic change compared to the solvation region and can be attributed to ionomer swelling.

4. Conclusions

The work presented investigates the water uptake, sorption mechanics and swelling characteristics of thin film Nafion and a commercially available Tokuyama AAEM ionomer from the vapour phase using a QCM.

The QCM frequency response has shown, as reported by other authors, that the water uptake is lower for the AAEM ionomer compared to that of Nafion at a given relative humidity. The active oscillation has also shown that unlike Nafion, the AAEM water uptake is not independent of film thickness.

Crystal admittance spectroscopy has been applied to this system for the first time to help better understand the sorption characteristics and swelling of Nafion and AAEM ionomers. The experimental results suggest some similarities in loading mechanisms between the two, albeit to varying magnitudes. Both the Nafion and AAEM ionomer exhibit a process of high viscoelasticity increases as ions within the ionomer are solvated. The results presented show that the Nafion solvation occurs at a significantly lower relative humidity and water uptake value compared to the AAEM ionomer; beyond the solvation period, the ionomer channels begin to adsorb water and swell. The Nafion ionomer exhibits significantly larger water uptake during the swelling regime, suggesting a superior swelling ratio than that of the AAEM.

Acknowledgements

The authors would like to acknowledge the NPL for supporting Bharath's PhD Studentship, the EPSRC for funding the Electrochemical Innovation Lab's fuel cell research programme through (EP/J016454/1; EP/K038656/1; EP/G060991/1; EP/J001007/1; EP/I037024/1; EP/G030995/1; EP/G04483X/1). PRS acknowledges the Royal Academy of Engineering for funding support.

References

[1] R.P. O'Hayre, Fuel Cell Fundamentals, 2nd ed, John Wiley & Sons, Hoboken, N.J, 2009.
[2] J. Larminie, A. Dicks, Fuel Cell Systems Explained, 2nd ed, J. Wiley, Chichester, West Sussex, 2003.
[3] T.J. Mason, J. Millichamp, T.P. Neville, P.R. Shearing, S. Simons, D.J.L. Brett, A study of the effect of water management and electrode flooding on the dimensional change of polymer electrolyte fuel cells, J. Power Sources 242 (2013) 70–77 , Nov 15.
[4] G.C. Abuin, M.C. Fuertes, H.R. Corti, Substrate effect on the swelling and water sorption of Nafion nanomembranes, J. Membr. Sci. 428 (2013) 507–515 , Feb 1.
[5] T.D. Gierke, G.E. Munn, F.C. Wilson, The morphology in nafion perfluorinated membrane products, as determined by wide-angle and small-angle X-ray studies, J. Polym. Sci. Part B – Polym. Phys. 19 (1981) 1687–1704.
[6] E.J. Roche, M. Pineri, R. Duplessix, A.M. Levelut, Small-angle scattering studies of nafion membranes, J. Polym. Sci. Part B-Polym. Phys. 19 (1981) 1–11.
[7] H.L. Yeager, A. Eisenberg, Perfluorinated ionomer membranes-introduction, ACS Sympos. Ser. 180 (1982) 1–6.
[8] K. Schmidt-Rohr, Q. Chen, Parallel cylindrical water nanochannels in Nafion fuel-cell membranes, Nat. Mater. 7 (2008) 75–83 , Jan.
[9] T.A. Zawodzinski, T.E. Springer, F. Uribe, S. Gottesfeld, Characterization of polymer electrolytes for fuel-cell applications, Solid State Ion. 60 (1993) 199–211 , Mar.
[10] T.A. Zawodzinski, C. Derouin, S. Radzinski, R.J. Sherman, V.T. Smith, T. E. Springer, S. Gottesfeld, Water-uptake by and transport through nafion (R) 117 membranes, J. Electrochem. Soc. 140 (1993) 1041–1047 , Apr.
[11] P. Krtil, A. Trojanek, Z. Samec, Kinetics of water sorption in Nafionthin films-Quartz crystal microbalance study, J. Phys. Chem. B 105 (2001) 7979–7983 , Aug 23.
[12] A. Kongkanand, Interfacial water transport measurements in nafion thin films using a quartz-crystal microbalance, J. Phys. Chem. C 115 (2011) 11318–11325 , Jun 9.
[13] D.L. Wood, J. Chlistunoff, J. Majewski, R.L. Borup, Nafion structural phenomena at platinum and carbon interfaces, J. Am. Chem. Soc. 131 (2009) 18096–18104 , Dec 23.
[14] M.A. Modestino, D.K. Paul, S. Dishari, S.A. Petrina, F.I. Allen, M.A. Hickner, K. Karan, R.A. Segalman, A.Z. Weber, Self-assembly and transport limitations in confined nafion films, Macromolecules 46 (2013) 867–873 , Feb 12.
[15] D.K. Paul, K. Karan, A. Docoslis, J.B. Giorgi, J. Pearce, Characteristics of self-assembled ultrathin nafion films, Macromolecules 46 (2013) 3461–3475 , May 14.
[16] S.K. Dishari, M.A. Hickner, Antiplasticization and water uptake of nafion thin films, ACS Macro Lett. 1 (2012) 291–295 , Feb.
[17] M.B. Satterfield, J.B. Benziger, Viscoelastic properties of nafion at elevated temperature and humidity, J. Polym. Sci. Part B – Polym. Phys. 47 (2009) 11–24 , Jan 1.
[18] C.W. Monroe, T. Romero, W. Merida, M. Eikerling, A vaporization-exchange model for water sorption and flux in Nafion, J. Membr. Sci. 324 (2008) 1–6 , Oct 31.
[19] Y. Tabuchi, R. Ito, S. Tsushima, S. Hirai, Analysis of in situ water transport in Nafion (R) by confocal micro-Raman spectroscopy, J. Power Sources 196 (2011) 652–658 , Jan 15.
[20] L. An, T.S. Zhao, Y.S. Li, Q.X. Wu, Charge carriers in alkaline direct oxidation fuel cells, Energy Environ. Sci. 5 (2012) 7536–7538 , Jun.
[21] J.R. Varcoe, M. Beillard, D.M. Halepoto, J.P. Kizewski, S.D. Poynton, R.C.T. Slade, Membrane and electrode materials for alkaline membrane fuel cells, Proton Exchange Membr. Fuel Cells 8, Pts 1 and 2 16 (2008) 1819–1834.
[22] J.R. Varcoe, P. Atanassov, D.R. Dekel, A.M. Herring, M.A. Hickner, P.A. Kohl, A. R. Kucernak, W.E. Mustain, K. Nijmeijer, K. Scott, T.W. Xu, L. Zhuang, Anion-exchange membranes in electrochemical energy systems, Energy Environ. Sci. 7 (2014) 3135–3191 , Oct.
[23] J.P. Kizewski, N.H. Mudri, R. Zeng, S.D. Poynton, R.C.T. Slade, J.R. Varcoe, Alkaline electrolytes and reference electrodes for alkaline polymer electrolyte membrane fuel cells, Polym. Electrolyte Fuel Cells 33 (1) (2010) 27–35.
[24] H. Yanagi, K. Fukuta, Anion exchange membrane and ionomer for alkaline membrane fuel cells (AMFCs), Proton Exchange Membr. Fuel Cells 8, Pts 1 and 2 16 (2008) 257–262.
[25] G. Merle, M. Wessling, K. Nijmeijer, Anion exchange membranes for alkaline fuel cells: a review, J. Membr. Sci. 377 (2011) 1–35 , Jul 15.
[26] Y.S. Li, T.S. Zhao, W.W. Yang, Measurements of water uptake and transport properties in anion-exchange membranes, Int. J. Hydrogen Energy 35 (2010) 5656–5665 , Jun.
[27] G. Sauerbrey, Verwendung von schwingquarzen zur wagung dunner schichten und zur mikrowagung, Z. Phys. 155 (1959) 206–222.
[28] M. Rodahl, F. Hook, A. Krozer, P. Brzezinski, B. Kasemo, Quartz-crystal microbalance setup for frequency and q-factor measurements in gaseous and liquid environments, Rev. Sci. Instrum. 66 (1995) 3924–3930 , Jul.
[29] D.A. Buttry, M.D. Ward, Measurement of interfacial processes at electrode surfaces with the electrochemical quartz crystal microbalance, Chem. Rev. 92 (1992) 1355–1379 , Sep–Oct.
[30] G. Liu, G. Zhang, QCM-D Studies on Polymer Behavior at Interfaces, Springer, New York, 2013.
[31] A. Cao-Paz, L. Rodriguez-Pardo, J. Farina, Temperature compensation of QCM sensors in liquid media, Sens. Actuators B – Chem. 193 (2014) 78–81 , Mar.
[32] S.J. Martin, V.E. Granstaff, G.C. Frye, Characterization of a quartz crystal microbalance with simultaneous mass and liquid loading, Analytical Chemistry 63 (1991) 2272–2281 , Oct 15.
[33] P. Vanysek, L.A. Delia, Impedance characterization of a quartz crystal

microbalance, Electroanalysis 18 (2006) 371–377 , Feb.
[34] W.G. Cady, Piezoelectricity: An Introduction to the Theory and Applications of Electromechanical Phenomena in Crystals, Dover Publications, New York, 1964, New rev. ed..
[35] H. Muramatsu, E. Tamiya, I. Karube, Computation of equivalent-circuit parameters of quartz crystals in contact with liquids and study of liquid properties, Anal. Chem. 60 (1988) 2142–2146 , Oct 1.
[36] R. Beck, U. Pittermann, K.G. Weil, Impedance analysis of quartz oscillators, contacted on one side with a liquid, Berichte Der Bunsen-Gesellschaft – Phys. Chem. Chem. Phys. 92 (1988) 1363–1368 , Nov.
[37] A.L. Kipling, M. Thompson, Network analysis method applied to liquid-phase acoustic-wave sensors, Anal. Chem. 62 (1990) 1514–1519 , Jul 15.
[38] M. Thompson, A.L. Kipling, W.C. Duncanhewitt, L.V. Rajakovic, B. A. Cavicvlasak, , Thickness-shear-mode acoustic-wave sensors in the liquid-phase-a review, Analyst 116 (1991) 881–890 , Sep.
[39] J.F. Rosenbaum, Bulk Acoustic Wave Theory and Devices, Artech House, Boston, 1988.
[40] J.L. Yan, M.A. Hickner, Anion exchange membranes by bromination of benzylmethyl-containing poly(sulfone)s, Macromolecules 43 (2010) 2349–2356 , Mar 9.
[41] J.R. Varcoe, R.C.T. Slade, Prospects for alkaline anion-exchange membranes in low temperature fuel cells, Fuel Cells 5 (2005) 187–200 , Apr.
[42] S. Chempath, J.M. Boncella, L.R. Pratt, N. Henson, B.S. Pivovar, Density functional theory study of degradation of tetraalkylammonium hydroxides, J. Phys. Chem. C 114 (2010) 11977–11983 , Jul 15.
[43] J. John, K.M. Hugar, J. Rivera-Melendez, H.A. Kostalik, E.D. Rus, H.S. Wang, G. W. Coates, H.D. Abruna, An electrochemical quartz crystal microbalance study of a prospective alkaline anion exchange membrane material for fuel cells: anion exchange dynamics and membrane swelling, J. Am. Chem. Soc. 136 (2014) 5309–5322 , Apr 9.
[44] T.A. Zawodzinski, T.E. Springer, J. Davey, R. Jestel, C. Lopez, J. Valerio, S. Gottesfeld, A comparative-study of water-uptake by and transport through ionomeric fuel-cell membranes, J. Electrochem. Soc. 140 (1993) 1981–1985 , Jul.
[45] C. Vallieres, D. Winkelmann, D. Roizard, E. Favre, P. Scharfer, M. Kind, On Schroeder's paradox, J. Membr. Sci. 278 (2006) 357–364 , Jul 5.
[46] L.M. Onishi, J.M. Prausnitz, J. Newman, Water-nafion equilibria: absence of Schroeder's paradox, J. Phys. Chem. B 111 (2007) 10166–10173 , Aug 30.
[47] J.R. Varcoe, R.C.T. Slade, E.L.H. Yee, S.D. Poynton, D.J. Driscoll, Investigations into the ex situ methanol, ethanol and ethylene glycol permeabilities of alkaline polymer electrolyte membranes, J. Power Sources 173 (2007) 194–199 , Nov 8.
[48] J.R. Varcoe, Investigations of the ex situ ionic conductivities at 30 degrees C of metal-cation-free quaternary ammonium alkaline anion-exchange membranes in static atmospheres of different relative humidities, Phys. Chem. Chem. Phys. 9 (2007) 1479–1486.
[49] D. Stoica, L. Ogier, L. Akrour, F. Alloin, J.F. Fauvarque, Anionic membrane based on polyepichlorhydrin matrix for alkaline fuel cell: synthesis, physical and electrochemical properties, Electrochim. Acta 53 (2007) 1596–1603 , Dec 31.
[50] G.C. Abuin, P. Nonjola, E.A. Franceschini, F.H. Izraelevitch, M.K. Mathe, H. R. Corti, , Characterization of an anionic-exchange membranes for direct methanol alkaline fuel cells, Int. J Hydrog. Energy 35 (2010) 5849–5854 , Jun.
[51] J.T. Hinatsu, M. Mizuhata, H. Takenaka, Water-uptake of perfluorosulfonic acid membranes from liquid water and water-vapor, J. Electrochem. Soc. 141 (1994) 1493–1498 , Jun.